Physics of the Earth and Planetary Interiors 188 (2011) 1–8

Contents lists available at ScienceDirect

Physics of the Earth and Planetary Interiors

journal homepage: www.elsevier.com/locate/pepi

The impact of variability in the rheological activation parameters on lower-mantle viscosity stratification and its dynamics

Ctirad Matyska [a], David A. Yuen [b], Renata M. Wentzcovitch [c], Hana Čížková [a,*]

[a] Department of Geophysics, Faculty of Mathematics and Physics, Charles University, V Holešovičkách 2, 180 00 Praha 8, Czech Republic
[b] Department of Geology and Geophysics and Minnesota Supercomputing Institute, University of Minnesota, 117 Pleasant Street, South East, 599 Walter Library, Minneapolis, MN 55455-0219, USA
[c] Chemical Engineering and Materials Science, University of Minnesota, 151 Amundson Hall, 421 Washington Ave. SE, Minneapolis, MN 55455-0219, USA

ARTICLE INFO

Article history:
Received 30 September 2010
Received in revised form 25 May 2011
Accepted 27 May 2011
Available online 7 June 2011

Keywords:
Lower-mantle dynamics
Activation parameters
Postperovskite (ppv) phase transition
Lower-mantle rheology
Radiative thermal conductivity
Plume clusters

ABSTRACT

The recently discovered spin-state crossover in iron in major mantle minerals at high pressures should exert dramatic influences on transport properties, such as the activation creep parameters in the deep mantle. Wentzcovitch et al. (2009) have computed the elastic parameter of ferropericlase that is affected by this crossover, the bulk modulus, at high realistic conditions, using first principles density functional theory plus Hubbard U. As a consequence of the spin crossover there is a significant softening of the bulk modulus and an attendant reduction of the activation energy in the creep law. Using a parameterized model capturing the basic physics, we have studied the dynamical consequences within the framework of a 2-D Cartesian convection model. Our models reveal a series of asthenospheres and are characterized first by a low-viscosity channel below the 670 km boundary ('second asthenosphere') caused by an increase of temperature and decrease in grain size reduction (superplascity) with the post-spinel transition, which results in partially layered convection. Further, the variability of the rheological parameters leads to the prevalent formation of viscosity minimum at a depth of about 1600 km ('third asthenosphere') caused by spin crossovers followed by a 'viscosity hill' in the bottom half of the lower mantle, the latter due to the increase of the activation energy in some low spin irons at the bottom of the mantle. Our numerical simulations reveal a tendency to the formation of small-scale convection below the 670 km boundary and bigger stabilized plumes – and/or plume clustering in the deep lower mantle. Other material properties at the bottom of the mantle (decrease of thermal expansivity, radiative thermal conductivity) also exert significant influence on the multi-scale lower-mantle plume dynamics.

1. Introduction

The dynamics of the lower mantle depends a great deal on material properties that are not well known but are generally believed to be greatly dependent on the pressure. These lower-mantle transport and thermodynamic properties – such as increased viscosity, increased lattice thermal conductivity, reduction in thermal expansivity due to increased pressure and also the radiative component of thermal conductivity (Matyska et al., 1994) are fundamental physical quantities, which result in the generation of superplumes and also, at the same time, other smaller scale dynamical features in the lower mantle (Hansen et al., 1993; Yuen et al., 1996; van Keken and Yuen, 1995; Matyska and Yuen, 2001, 2005, 2006, 2007; Deschamps et al., 2007; Tackley et al., 2007). Since the first attempt by McKenzie (1966), where a very high viscosity was predicted for the lower mantle based on the Earth's rotational shape, the viscosity stratification of the lower mantle has been fraught with some uncertainties. For over three decades the lower mantle was thought to have a relatively constant viscosity (Cathles, 1975; Peltier and Andrews, 1976; Hager et al., 1985; King and Masters, 1992), until the issue of multiplicity of lower-mantle viscosity solutions was raised concerning the rotational data (Sabadini et al., 1982; Yuen and Sabadini, 1985) in which a higher lower-mantle viscosity of 10^{22} to 10^{23} Pas was allowed. The notion of a 'viscosity hill' in the middle of the lower mantle was first developed by Ricard and Wuming (1991) from modeling the dynamic geoid and topography. This idea was further reinforced from both geoid and post-glacial rebound inversion by Forte and Mitrovica (2001) and Mitrovica and Forte (2004), Tosi et al. (2005) or recently by Soldati et al. (2009). However, a real physical explanation still remained elusive for a long time.

Recently, the high-to-low spin crossover in ferrous iron in ferropericlase (e.g. Badro et al., 2003; Lin et al., 2005, 2007a; Goncharov et al., 2006; Kantor et al., 2006; Tsuchiya et al., 2006a; Crowhurst et al., 2008; Lin and Tsuchiya, 2008; Wentzcovitch et al., 2009;

* Corresponding author. Tel.: +420 2 21912544; fax: +420 2 21912555.
E-mail address: Hana.Cizkova@mff.cuni.cz (H. Čížková).

0031-9201/$ - see front matter © 2011 Elsevier B.V. All rights reserved.
doi:10.1016/j.pepi.2011.05.012

Wu et al., 2009; Hsu et al., 2010) and in ferrous and ferric irons in perovskite (McCammon, 1997; Badro et al., 2004; Frost et al., 2004; Li et al., 2004, 2006; Jackson et al., 2005; McCammon et al., 2008; Lin et al., 2008; Hofmeister, 2006; Zhang and Oganov, 2006; Stackhouse et al., 2007; Bengtson et al., 2008, 2009; Umemoto et al., 2008, 2010; Hsu et al., 2010, 2011; Catalli et al., 2010; Bower et al., 2009; Shahnas et al., 2011) have been extensively investigated by experiments, theory and dynamic modeling. Some of these studies have been able to address thermoelastic properties of these minerals at relevant pressure (P) and temperature (T) conditions (Lin et al., 2007b; Tsuchiya et al., 2006b; Wentzcovitch et al., 2009; Wu et al., 2009; Hsu et al., 2011) and there is clearly a bulk modulus softening during the spin crossover. Combining from first principles total energy calculations with classical elastic deformation theory Wentzcovitch et al. (2009) computed thermoelastic properties of ferropericlase. Preliminary results by Hsu et al. (2011) indicate similar effects along the spin crossover in perovskite in the same pressure range in the mantle. Shear and bulk sound wave velocities can be related to the activation energy G^* (e.g. Sammis et al., 1977), which has traditionally been taken to be a monotonically increasing function (e.g. Ranalli, 1995; Karato, 2008) and has been employed exclusively in mantle convection modeling (e.g. Schubert et al., 2001). Consequently, the viscosity η can be assumed as a thermally activated process in the Arrhenius sense

$$\eta = A \exp\left(\frac{G^*}{RT^*}\right), \tag{1}$$

where the prefactor A is a constant for a Newtonian fluid, R is the universal gas constant and T^* is the absolute temperature. Although ferropericlase is not the most abundant lower-mantle mineral, it probably controls lower-mantle deformations because of its relative softness (Zerr and Boehler, 1994; Yamazaki and Karato, 2001; Holtzman et al., 2005; Larkin et al., 2005; Wentzcovitch et al., 2009). The additional spin crossover in ferric iron in perovskite (Catalli et al., 2010; Hsu et al., 2011) should contribute to make the non-monotonicity in activation parameters even more a poignant issue.

Further clarification of activation parameters behavior and related micro/meso scale mechanisms related with plasticity in the spin crossover regime at mantle conditions is desirable. In particular, a first principles calculation of diffusion rates of high-spin and low-spin ferrous iron in periclase (Ammann et al., 2011) does not confirm the notion of reduced activation parameters. Deformation at the high temperatures and low stresses typical of the lower mantle should occur by diffusion creep and this type of calculation generally offers good insights on activation parameters for diffusion creep. However, the phenomenon of spin crossover is essentially a state change in a broad pressure range in a certain sense, resembling the two phase loop of a structural transformation. It is well known that during phase changes involving volume reduction, the bulk modulus softens and longitudinal velocities decrease (Li and Weidner, 2008). Also, visco-plastic deformation is observed during the transformation if subjected to stress perturbations with periods comparable to the transformation relaxation time. In the case of the olivine-ringwoodite system in the two-phase loop regime, the Q factor reduces to 5 for cyclic loads with periods 1000 s. Although relaxation times for spin crossovers should be short, stress relaxation is not simply accommodated by diffusion creep, but also by a continuous change in spin populations and/or configurations. Therefore, the deformation mechanism during spin state change should be more complex than simple diffusion creep, very likely involving also an anelastic component unrelated with diffusion but related with elasticity. In this situation, the elastic strain energy model should capture the essence of this phenomenon. In fact, deformation experiments at room temperature up to 81 GPa in ferropericlase (Lin et al., 2009), indicate a reduction in the strength of ferropericlase in the regime of the spin crossover. Deformation at room temperature under relatively large stresses should occur by dislocation creep, as opposed to by diffusion creep, therefore these results do not translate directly to deformation in the deep mantle. Nevertheless the reduction in strength in the mixed spin regime observed by Lin et al. (2009), supports the notion of a reduction in strength and therefore viscosity during spin crossovers in the mantle.

The main purpose of this paper is to demonstrate the dynamical influences exerted by the viscosity variations due to the possible non-monotonic behavior of the activation energy with depth and also horizontal temperature variations in the lower mantle. The main idea of the viscosity behavior due to the variability of activation energy with depth is illustrated in Fig. 1 – viscosity variations are very sensitive to both the activation energy G^* and local temperature field and thus even a relatively shallow local minimum of G^* can result in a substantial minimum of viscosity. Temperature gradients in both the vertical and horizontal directions are then important control parameters in determining the viscosity structure in the lower mantle. In the rest of the paper we will also discuss the role played by potential changes of local properties in the D''-layer on lower-mantle dynamics.

2. Model description

We have employed a two-dimensional Cartesian model for thermal convection in which the dimensionless stream function and temperature in the extended-Boussinesq approximation (e.g. Steinbach et al., 1989) are employed. The details of this model can be found in (Matyska and Yuen, 2007). We note that the mantle phase changes are set at a given depth within the framework of the effective thermal expansivity formulation (Christensen and Yuen, 1985). The Rayleigh number $Ra \equiv \rho_s^2 c_p \alpha_s \Delta T g d^3/\eta_{ref} k_s = 10^7$, ($\rho_s$ is the surface density, α_s is the surface thermal expansivity, ΔT is the temperature drop across the mantle, g is the gravity acceleration, d is the depth of the mantle used in the non-dimensionalization, c_p is the specific heat under a constant pressure, η_{ref} is a reference viscosity and k_s is the surface thermal conductivity). The dimensionless internal heating $R \equiv Qd^2/k_s\Delta T = 3$, where Q denotes volumetric heat sources, which corresponds approximately to one fourth of the whole mantle chondritic heating (e.g. Leitch and Yuen, 1989) because of our Cartesian geometry (O'Farrell and Lowman, 2010). Finally, the surface dissipation number Di used for adiabatic and viscous heatings $Di = \alpha_s g d/c_p = 0.5$ was chosen.

At a dimensionless depth $z = 0.23$, corresponding to a depth of 670 km, endothermic spinel-perovskite phase change was incorporated into all models by means of the buoyancy parameter $P = (\Delta\rho/\alpha_s\rho^2 g d)(dp/dT)$ equal to -0.08(ρ is a reference mantle density, $\Delta\rho$ is the density jump due to the phase change under consideration and dp/dT is the Clapeyron slope). The post-perovskite phase change near the core-mantle boundary at a depth $z = 0.92$, corresponding to a depth of 2680 km, with $P = 0.05$ was considered in the cases, when the ppv phase transition in the D''-layer was taken into account. Computations have been performed in a wide box with an aspect ratio equal to ten. One hundred twenty-nine evenly spaced points were employed in the vertical direction and the same resolution was used in the horizontal direction.

The dimensionless thermal expansivity profile decreasing with depth has been parameterized to

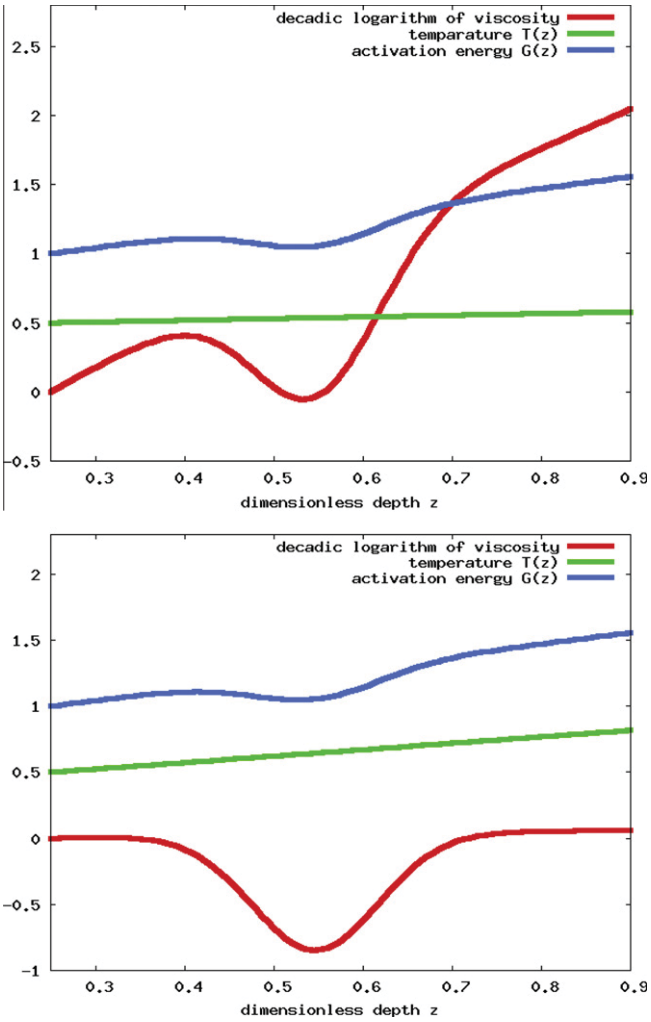

Fig. 1. Schematic illustration of the effect of non-monotonic depth profile of activation energy $G(z)$ to the depth profile of the viscosity. Blue line represents the activation energy profile, green line shows the geotherm and red line is the resulting viscosity profile computed by means of Eq. (3). The upper and lower panels differ in the geotherm – the upper panel is for a relatively flat geotherm, while the lower panel has a steeper temperature gradient. In both cases a relatively shallow minimum of the activation energy produces rather deep viscosity minimum but lower temperature gradient is needed to obtain a 'viscosity hill' above the CMB. (For interpretation of the references in colour in this figure legend, the reader is referred to the web version of this article.)

$$\begin{aligned} \frac{\alpha}{\alpha_s} &= (1+0.78z)^{-5} && \text{if} \quad 0 \leqslant z \leqslant 0.23, \\ \frac{\alpha}{\alpha_s} &= 0.44(1+0.35(z-0.23))^{-7} && \text{if} \quad 0.23 < z \leqslant 1, \end{aligned} \tag{2}$$

which corresponds to Anderson–Grüneisen parameter of the upper-mantle (lower-mantle) minerals close to 5 (7), which is in accord with the estimates for olivine (Chopelas and Boehler, 1992) and perovskite (Katsura et al., 2009).

The viscosity formula (1) was rewritten into the dimensionless quantities, which resulted in the relation

$$\frac{\eta}{\eta_{ref}} = \exp\left(12.66\left(\frac{G(z)}{0.15+1.7T}-1\right)\right), \tag{3}$$

where T is the dimensionless temperature equal to 0 at the surface ($z=0$) and equal to 1 at the CMB ($z=1$). Finally, we have approximated the non-monotonic depth-dependence of the activation energy (Wentzcovitch et al., 2009; Morra et al., 2010) by a simple piece-wise linear function

$$\begin{aligned} G(z) &= 1.0 && \text{for} \quad 0.00 \leqslant z \leqslant 0.23, \quad (a) \\ G(z) &= 1.0 + 0.2(z-0.23)/0.19 && \text{for} \quad 0.23 \leqslant z \leqslant 0.42, \quad (b) \\ G(z) &= 1.2 - 0.1(z-0.42)/0.13 && \text{for} \quad 0.42 \leqslant z \leqslant 0.55, \quad (c) \\ G(z) &= 1.1 + 0.7(z-0.55)/0.45 && \text{for} \quad 0.55 \leqslant z \leqslant 1.00 \quad (d) \end{aligned} \tag{4}$$

and we have employed this parameterization in most of the models. The employed viscosity formula (3) yields a strong temperature dependence of viscosity. Without any additional creep mechanism (e.g. the stress-dependent Peierls creep) such a temperature-dependence of viscosity produces a stagnant high-viscosity lid at the surface. In order to obtain sluggish motions in the upper-boundary thermal layer, we have confined the viscosity changes in the upper mantle to only $\mp$ two orders of magnitude. From the numerical reasons we also have to bound the viscosity variations in the lower mantle to $\mp$ three orders of magnitude, which is, however, sufficient for producing both high-viscosities at a depth corresponding to the 'viscosity hill' and low viscosities inside hot uprising plumes.

3. Results

We have started with the case, where the depth-dependence of activation energy $G(z)$ is given by Eq. (4), no ppv is considered in the D''-layer and only the constant phonon thermal conductivity is taken into account for the entire mantle (Fig. 2). In this case we have obtained nearly steady-state convection. Huge very stable cold downwellings with unrealistic thicknesses and big plumes with the heads barely reaching close to 670 km boundary are present in the lower mantle. Such a steady-state with extremely thick cold downwellings that are created as a result of relatively low temperature in the lower mantle can thus hardly be consistent with real mantle convection and it becomes clear that other physical processes are needed to obtain geophysically more realistic scenarios.

First, we added the post-perovskite (ppv) transition into the D''-layer. It is well established that the exothermic perovskite–post-perovskite phase change increases the chaotic time-dependence of mantle convection (Matyska and Yuen, 2006; Nakagawa and Tackley, 2004). In this study we focus entirely on the dynamics of the lower mantle and will not be concerned with the upper-mantle convection. It is of interest that after reaching a statistical equilibrium one can obtain both a big plume similar to the plumes generated in the previous case (see the left part of panels in Fig. 3) and plume clusters with intensive plume–plume interactions within the framework of one dynamical model. It is remarkable that the plume clusters are visible more or less only in the bottom half of the lower mantle and only some plume heads penetrate through the lower-mantle viscosity barrier. These heads are sometimes drifted horizontally by a mean flow below the 670 km boundary of the opposite direction to the mean flow in the D''-layer, which induces drifts in the roots of these plumes. The plume limbs can be thus substantially inclined. We should note here, that similar

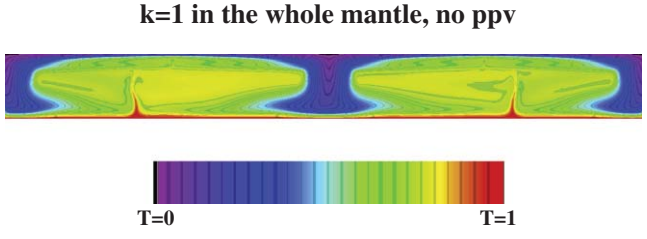

Fig. 2. One snapshot of the dimensionless temperature field for the model with activation energy $G(z)$ shown in Eq. (4), with constant thermal conductivity and without ppv phase transition.

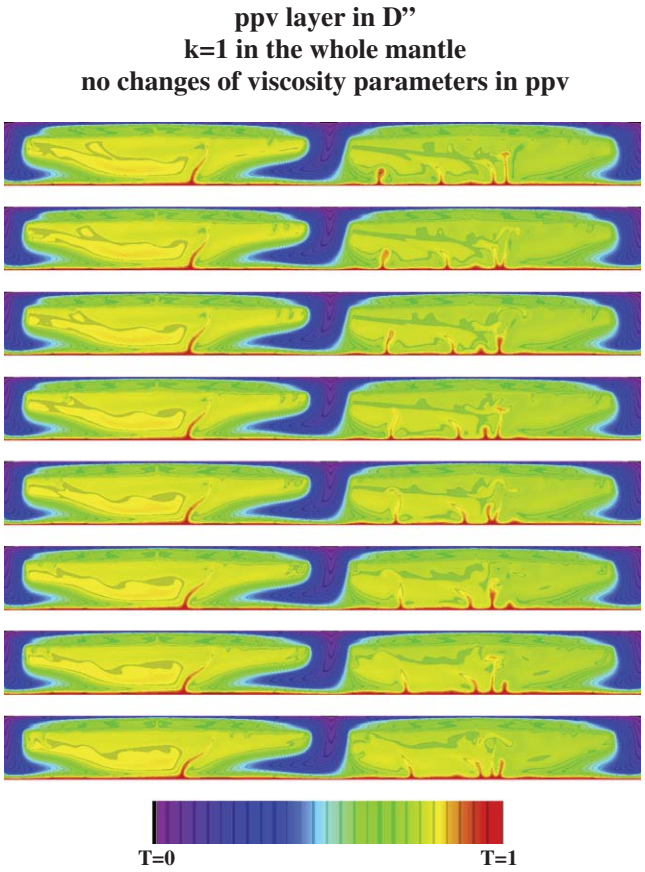

Fig. 3. The dimensionless temperature field for a model with the same $G(z)$ as in Fig. 2 and with a perovskite to postperovskite phase change. Thermal conductivity is constant throughout the whole mantle.

to the previous model shown in Fig. 2, we get here again very thick cold downwellings as the result of the temperature-dependent viscosity. Although thicker downwelling structures in the lower mantle are expected (Běhounková and Čížková, 2008), it is clear that we need to take into account additional mechanisms, that are able to promote heat transfer in the lower mantle.

Radiative transfer of heat is another physical mechanism that can be present close to the core–mantle boundary CMB (Badro et al., 2004; Hofmeister, 2008; Keppler et al., 2008; Goncharov et al., 2009). If the radiative thermal conductivity in the D''-layer is comparable with the phonon thermal conductivity (or is even higher), its influence to the lower-mantle dynamics can be substantial (Matyska and Yuen, 2005, 2006, 2007; Naliboff and Kellogg, 2006). This is the reason why we also added the dimensionless thermal conductivity in the form

$$k = 1 + T^3 \tag{5}$$

into the D''-layer to test the case when the magnitude of the radiative thermal conductivity is the same as that of the phonon thermal conductivity at the CMB. One can clearly recognize in Fig. 4a that the lower mantle becomes hotter and the cold downwellings are thus thinned. Moreover, plume clusters – see also (Schubert et al., 2004) – in the bottom half of the lower mantle can be again created but the middle of the lower mantle seems to act as 'a barrier' for the smaller uprising plumes formed in the plume cluster. From the physical point of view, the important role is probably played by the low viscosity channel at the mid-mantle corresponding to the

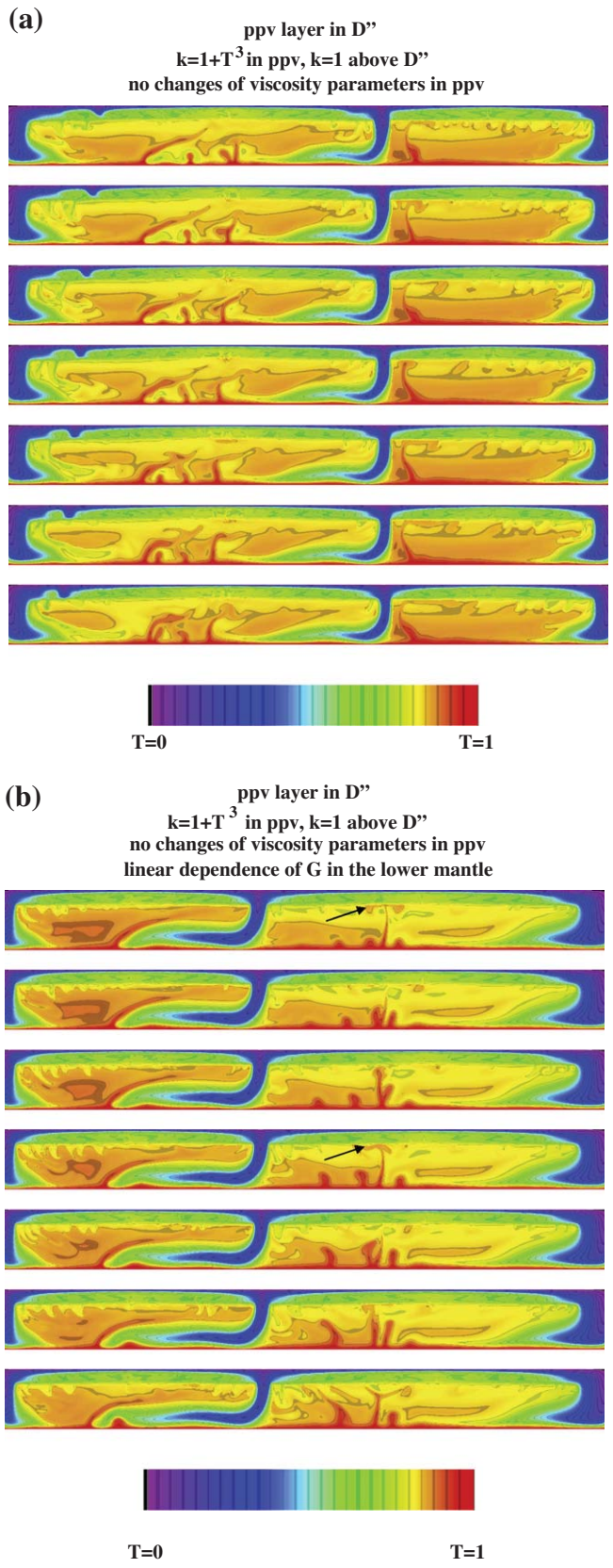

Fig. 4. (a) Snapshots of the dimensionless temperature field for a model with the same $G(z)$ as in Fig. 2, with a perovskite to postperovskite phase change and a temperature-dependent thermal conductivity in ppv. (b) The same, but now for linearly increasing $G(z)$. Black arrows indicate the positions of the hot anomalies below the 670 km boundary.

local minimum of $G(z)$, which facilitates lateral flows, see Fig. 7. Moreover, higher temperature results in a decrease of viscosity at the CMB (see also Figs. 7 and 8), which also promotes lateral flow with long wavelength. As this model, where an increase of thermal conductivity at the bottom of the mantle is included, generate more reasonable convection patterns than the two previous models, we have decided to deal with more details concerning the influence of viscosity changes within the framework of the models with such an increased thermal conductivity. First, we tried to test sensitivity of convection pattern to a shift of local maximum and minimum of the activation energy G by means of the formula.

$$\begin{aligned} G(z) &= 1.0 && \text{for} \quad 0.00 \leqslant z \leqslant 0.23, && (a)\\ G(z) &= 1.0 + 0.2(z-0.23)/0.12 && \text{for} \quad 0.23 \leqslant z \leqslant 0.35, && (b)\\ G(z) &= 1.2 - 0.1(z-0.35)/0.30 && \text{for} \quad 0.35 \leqslant z \leqslant 0.65, && (c)\\ G(z) &= 1.1 + 0.7(z-0.65)/0.35 && \text{for} \quad 0.65 \leqslant z \leqslant 1.00. && (d) \end{aligned} \tag{6}$$

This shift was chosen more or less arbitrarily just to get an idea about its influence. Note that the slopes of $G(z)$ are perturbed by more than 25% as a result of this shift. However, the result of this change of G to convection pattern and temperature distribution is not substantial. The question thus arises, whether the traditional linear increase of G with pressure generate similar results or not. This was the reason, why we have also computed the model, where $G(z)$ increases linearly from 1 for $z = 0.23$ to 1.8 for $z = 1$, see Fig. 4b. Again, both single plumes as well as plume clusters can be generated but the non-existence of a low-viscosity channel in the mid-mantle results in bigger plumes with heads reaching regularly the interface at 670 km and creating thus very hot broad anomalies (see black arrows). It is a matter of debate, whether such broad hot anomalies below the 670 km are/were present in the real Earth.

As there are speculations that viscosity of the ppv could be substantially lower than the viscosity of perovskite (Yamazaki et al., 2006; Čížková et al., 2010; Hunt et al., 2009; Tosi et al., 2009; Ammann et al., 2010), we also tested separately the case, where the viscosity of ppv was lowered by a factor of 10 with respect to formula (3). Radiative transfer of heat was not considered in this model. One can see in Fig. 5 that the results are very similar to those from the previous model, i.e., a decrease of the viscosity in the D''-layer can cause similar dynamical effects as an increase of the thermal conductivity. However, lower-boundary layer instabilities are able to produce also very small plumes. The mean flow in

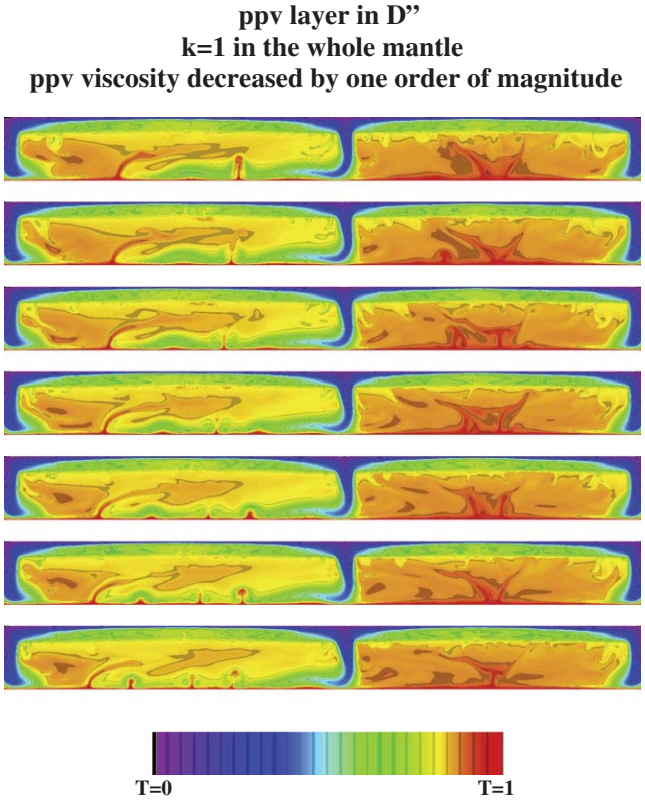

Fig. 5. Snapshots of the dimensionless temperature field for a model with the same $G(z)$ as in Fig. 2 and with a perovskite to postperovskite phase change. Thermal conductivity is constant throughout the whole mantle. The viscosity is decreased by a factor of 10 in ppv.

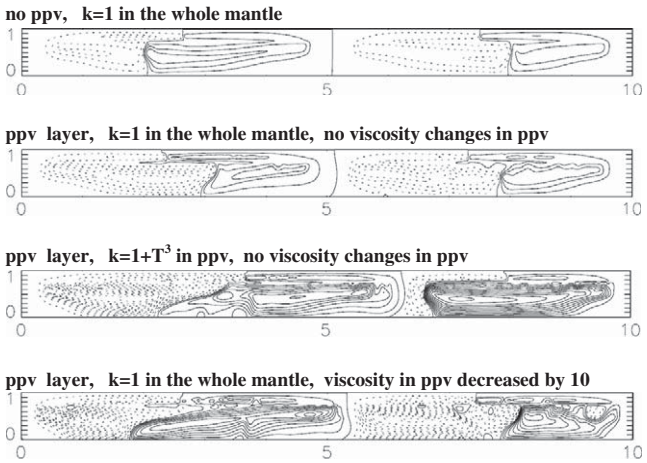

Fig. 6. Stream function for the models shown in Figs 2–5. Solid lines correspond to clock-wise motion, dashed lines indicate anti-clock-wise motion. We call attention to the complex multiscale circulatory patterns in the bottom two panels in contrast to the topmost panel.

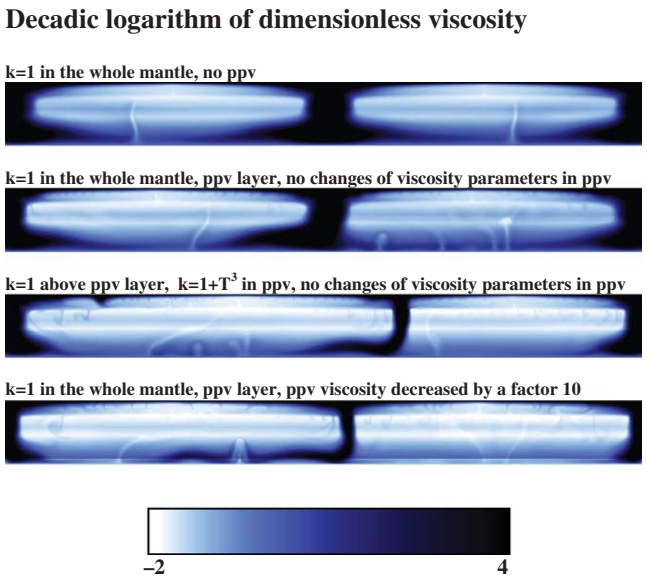

Fig. 7. The viscosity distribution in the four studied models with the $G(z)$ given by Eq. (4): 1. model without ppv, 2. model with ppv and constant thermal conductivity, 3. model with temperature dependent thermal conductivity in the ppv, 4. model with constant thermal conductivity and low ppv viscosity. Decadic logarithm of dimensionless viscosity is shown. We draw attention to the white strips in the lower mantle representing the second and third asthenospheres.

the upper half of the lower mantle is then the reason why the heads of the plumes are drifted laterally.

The comparison of streamlines for the four above mentioned models (Fig. 6) demonstrates the sensitivity of the flow field to the changes of the parameters. Clearly, the complex parameters of the D''-layer (higher k or lower η) enhance the vigor of convection and result in multiscale structures. The plot of a 2-D viscosity distribution corresponding to the four studied cases (Fig. 7) clearly shows the presence of the distinct low-viscosity layers (white color) in the upper half of the lower mantle. The vertical viscosity contrast associated with these layers is comparable to the horizontal viscosity contrast between the plumes and the ambient mantle. In the lower mantle we observe two low-viscosity layers – one below the 670 km ('second asthenosphere') is created by a high superadiabatic temperature gradient caused by a partial layering of the flow and the other one in the mid-mantle ('third asthenosphere') associated with the minimum of the activation energy.

Fig. 8 shows the horizontally averaged temperatures and their corresponding vertical viscosity profiles for all model runs with activation energy parameterization according to Eq. (4). We should note the remarkable subadiabatic temperature gradient obtained in all calculations above the D''-layer. This can be attributed to the presence of the large scale cold anomalies stored at the bottom of the mantle. The main physical consequence effect is the presence of a 'viscosity hill' at the bottom of the mantle, which is very sensitive to the horizontally averaged temperature (see also Fig. 1), i.e. to the material properties of the deep mantle and the D''-layer structure. Further information on such a 'viscosity hill' in the deep mantle coming from postglacial rebound and dynamic geoid modeling (e.g. Mitrovica and Forte, 2004) may provide an independent constraint on lower-mantle temperatures and consequently the material properties.

4. Concluding remarks

The non-monotonic behavior of the activation energy, caused by high spin to low-spin crossovers of both periclase and perovskite (Wentzcovitch et al., 2009; Hsu et al., 2011), should be reflected in the rather complex viscosity variations in the lower mantle. In its upper half we have two viscosity minima. The first minimum below the 670 km boundary is caused by an increase

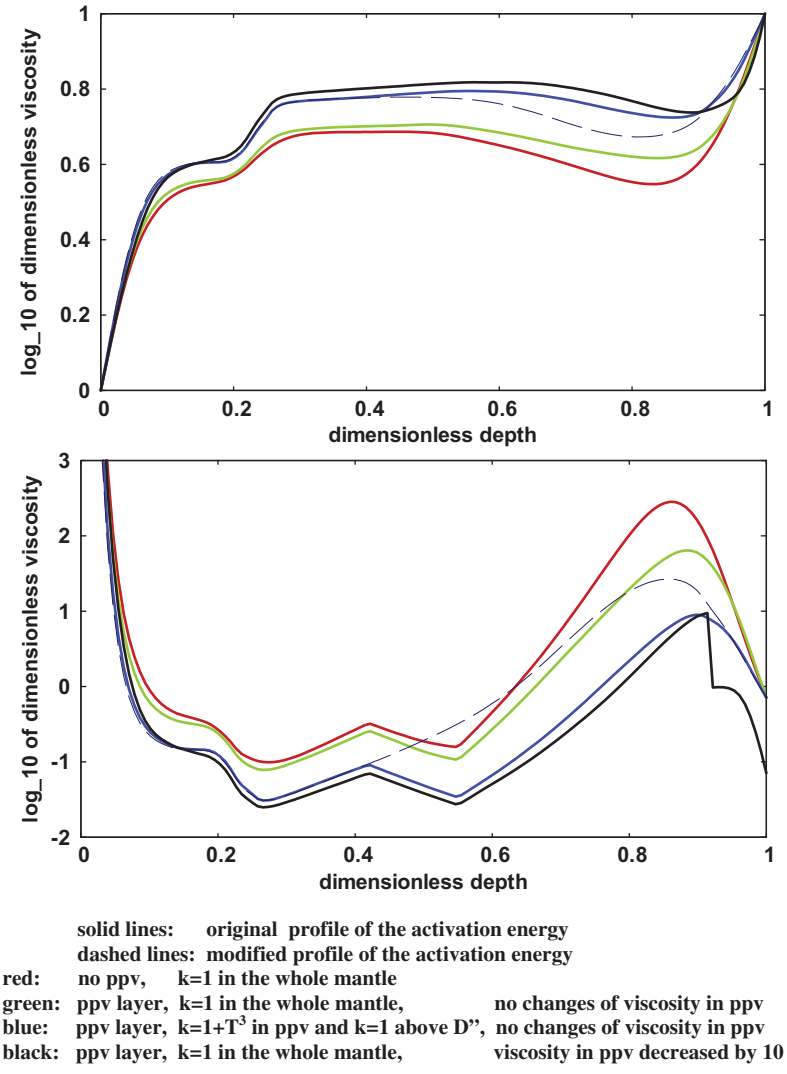

Fig. 8. Horizontally averaged temperatures (upper panel) and corresponding viscosity profiles (lower panel) for the four studied models: model without ppv with constant thermal conductivity (red line), model with ppv and constant thermal conductivity (green line), model with temperature dependent thermal conductivity in ppv (blue line) and model with low ppv viscosity and constant thermal conductivity (black line). Thick lines are for the reference activation energy $G(z)$ parameterization (Eq. (4)), thin line is for the linearly increasing activation energy in the lower mantle. (For interpretation of the references in colour in this figure legend, the reader is referred to the web version of this article.)

in the local temperature due to deflected plumes at the 670 km transition. Its presence has already been pointed out by, e.g., Kido and Čadek (1997) on the basis of the geoid inversions and it is usually denoted as a 'second asthenosphere'. The second minimum ('third asthenosphere') found at a depth of about 1600 km corresponds to a region of low activation energies caused by spin crossovers in ferropericlase and perovskite (Figs. 7 and 8). These two minima are followed by a 'viscosity hill' above the D''-layer. Such a feature has been, e.g., inferred by Ricard and Wuming (1991) in the inversion of the geoid, topography and plate motions and by the joint inversion of geoid and postglacial rebound (Forte and Mitrovica, 2001; Mitrovica and Forte, 2004). Finally, there is a viscosity minimum at the CMB generated by a temperature increase and/or intrinsic low viscosity of the ppv (Yamazaki et al., 2006; Čížková et al., 2010; Hunt et al., 2009; Tosi et al., 2009; Ammann et al., 2010).

The plume dynamics in the lower mantle on all scales is influenced by these complexities of the viscosity variations and also by the presence of the ppv. The latter provides additional influential properties, such as lower intrinsic viscosity (Yamazaki et al., 2006; Čížková et al., 2010; Hunt et al., 2009; Tosi et al., 2009; Ammann et al., 2010) and higher thermal conductivity. The presence of the perovskite to postperovskite exothermic phase change increases the lower-mantle temperature and thus decreases the maximum viscosity by about a factor of 5. Further reduction of the viscosity hill above the CMB is observed, if the ppv layer is characterized either by the increased thermal conductivity or lower viscosity. In both cases the efficiency of the heat transport from the core is enhanced and the lower-mantle viscosity is thus decreased through its thermal dependence. The overall reduction in the viscosity hill with respect to the model without ppv could thus be even more than one order of magnitude.

While the model without ppv phase transition is characterized by stable vertical plumes and very thick cold downellings, including the exothermic phase change above the CMB enhances the activity of plumes and enforces the plume-plume interactions, which leads to clustering and plume bending. Both the decrease of the ppv viscosity and increase of the thermal conductivity result in yet more vigorous plume motions and the bending of plumes from the large-scale circulation is observed (Tarduno et al., 2009). Thus the plumes inclined under relatively steep angle are typical features found in these models. This type of behavior is caused by the existence of the large-scale horizontal flow in the unstable lower thermal-boundary layer in combination with the viscosity hill and counter-horizontal flow enabled by the existence of the second and third asthenosphere. Increased vigor of convection in the lower mantle due to a potential increase of thermal conductivity and/or decrease of viscosity in the D''-layer due to the presence of ppv results in appearance of small-scale convection in the second asthenosphere (e.g. Kido and Čadek, 1997) right below the transition zone. These small-scale flow patterns in the lower mantle may influence the local mixing of geochemical anomalies and appearance of secondary plumes in the upper mantle. Note here that small upper-mantle plumes are generated at 670 km interface in our models and we do not observe long plumes originating from D'' with the heads below the lithosphere. However, some small upper-mantle plumes can be fed from the lower-mantle plume heads below the 670 km.

Acknowledgements

We thank Nicola Tosi and Johnny Justo for inspiring discussions about lower-mantle rheology and Scott King, Masaki Yoshida and an anonymous reviewer for constructive comments on the manuscript. This research has been supported by the Czech Science Foundation Grant P210/11/1366 and by the Research Project MSM0021620860 of the Czech Ministry of Education and US NSF Grants to Vlab and CMG Collaboration.

References

Ammann, M.W., Brodholt, J.P., Wookey, J., Dobson, D.P., 2010. First-principles constraints on diffusion in lower-mantle minerals and a weak D'' layer. Nature 465, 462–465.

Ammann, M.W., Brodholt, J.P., Dobson, D.P., 2011. Ferrous iron diffusion in periclase across the spin transition. Earth Planet. Sci. Lett. 302, 393–402.

Badro, J., Fiquet, G., Guyot, F., Rueff, J.-P., Struzhkin, V.V., Vankó, G., Monaco, G., 2003. Iron partitioning in Earth's mantle: toward a deep lower mantle discontinuity. Science 300, 789–791.

Badro, J., Rueff, J.-P., Vanko, G., Monaco, G., Fiquet, G., Guyot, F., 2004. Electronic transitions in perovskite: possible non-convecting layers in the lower mantle. Science 305, 383–386.

Běhounková, M., Čížková, H., 2008. Long-wavelength character of subducted slabs in the lower mantle. Earth Planet. Sci. Lett. 275, 43–53.

Bengtson, A., Persson, K., Morgan, D., 2008. Ab initio study of the composition dependence of the pressure-induced spin crossover in perovskite (Mg1–xFex)SiO_3. Earth. Planet. Sci. Lett. 265, 535–545.

Bengtson, A., Li, J., Morgan, D., 2009. Mossbauer modeling to interpret the spin state of iron in (Mg,Fe)SiO_3 perovskite. Geophys. Res. Lett. 36, L15301.

Bower, D.J., Gurnis, M., Jackson, J.M., Sturhahn, W., 2009. Enhanced convection and fast plumes in the lower mantle induced by the spin transition in ferropericlase. Geophys. Res. Lett. 36, L10306.

Catalli, K., Shim, S.H., Prakapenka, V.B., Zhao, J.Y., Sturhahn, W., Chow, P., Xiao, Y.M., Liu, H.Z., Cynn, H., Evans, W.J., 2010. Spin state of ferric iron in $MgSiO_3$ perovskite and its effect on elastic properties. Earth Planet. Sci. Lett. 289, 68–75.

Cathles, L.M., 1975. The Viscosity of the Earth's Mantle. Princeton University Press, Princeton, p. 386.

Čížková, H., Čadek, O., Matyska, C., Yuen, D.A., 2010. Implications of post-perovskite transport properties for core-mantle dynamics. Phys. Earth Planet. Int.. doi:10.1016/j.pepi.2009.08.008.

Chopelas, A., Boehler, R., 1992. Thermal expansivity in the lower mantle. Geophys. Res. Lett. 19, 1983–1986.

Christensen, U., Yuen, D.A., 1985. Layered convection induced by phase transitions. J. Geophys. Res. 90, 10291–10300.

Crowhurst, J.C., Brown, J.M., Goncharov, A.F., Jacobsen, S.D., 2008. Elasticity of (Mg,Fe)O through the spin transition of iron in the lower mantle. Science 319, 451–453.

Deschamps, F., Trampert, J., Tackley, P.J., 2007. Thermo-chemical structure of the lower mantle: seismological evidence and consequences for geodynamics. In: Yuen, D.A., Maruyama, S., Karato, S.-I., Windley, B.F. (Eds.), Superplumes: Beyond Plate Tectonics. Springer, pp. 293–320.

Forte, A.M., Mitrovica, J.X., 2001. Deep-mantle high-viscosity flow and thermochemical structure inferred from seismic and geodynamic data. Nature 410, 1049–1056.

Frost, D.J., Liebske, Ch., Langenhorst, F., McCammon, C., Trnnes, R., Rubie, D., 2004. Experimental evidence for the existence of iron-rich metal in the Earth's lower mantle. Nature 428, 409.

Goncharov, A.F., Struzhkin, V.V., Jacobsen, S.D., 2006. Reduced radiative conductivity of low-spin (Mg,Fe)O in the lower mantle. Science 312, 1205–1208.

Goncharov, A.F., Beck, P., Struzhkin, V.V., Haugen, B.D., Jacobsen, S.D., 2009. Thermal conductivity of lower mantle minerals. Phys. Earth Planet. Inter. 174, 24–32.

Hager, B.H., Clayton, R.W., Richards, M.A., Comer, R.P., Dziewonski, A.M., 1985. Lower mantle heterogeneity, dynamic topography and the geoid. Nature 313, 541–546.

Hansen, U., Yuen, D.A., Kroening, S.E., Larsen, T.B., 1993. Dynamical consequences of depth-dependent thermal expansivity and viscosity on mantle circulations and thermal structure. Phys. Earth Planet. Inter. 77, 205–223.

Hofmeister, A., 2006. Is low-spin Fe^{2+} present in Earth's mantle? Earth Planet. Sci. Lett. 243, 44.

Hofmeister, A.M., 2008. Inference of high thermal transport in the lower mantle from laser-flash experiments and the damped harmonic oscillator model. Phys. Earth Planet. Int. 170, 201–206.

Holtzman, B.K., Kohlstedt, D.L., Morgan, J.P., 2005. Viscous energy dissipation and strain partitioning in partially molten rocks. J. Petrol. 46, 25692592.

Hsu, H., Umemoto, K., Wu, A., Wentzcovitch, R.M., 2010. Spin-state crossover of iron in lower-mantle minerals: results of DFT+U investigations. Rev. Mineral. Geochem. 71, 96–199.

Hsu, H., Blaha, P., Cococcioni, M., Wentzcovitch, R., 2011. Spin state crossover and hyperfine interactions of ferric iron in $MgSiO_3$ perovskite. Phys. Rev. Lett. 106, 118501.

Hunt, S.A., Weidner, D.J., Liping Wang, L.L., Walte, N.P., Brodholt, J.P., Dobson, D.P., 2009. Weakening of calcium iridate during its transformation from perovskite to post-perovskite. Nature Geosci. 2, 794–797.

Jackson, J.M., Sturhahn, W., Shen, G.Y., Zhao, J.Y., Hu, M.Y., Errandonea, D., Bass, J.D., Fei, Y.W., 2005. A synchrotron Mossbauer spectroscopy study of (Mg,Fe)SiO_3 perovskite up to 120 GPa. Am. Mineral. 90, 199–205.

Kantor, I.Y., Dubrovinsky, L.S., McCammon, C.A., 2006. Spin crossover in (Mg,Fe)O: a Mossbauer effect study with an alternative interpretation of X-ray emission spectroscopy data. Phys. Rev. B 73, 100101.

Karato, S.-I., 2008. Deformation of Earth Materials: An Introduction to the Rheology of Solid Earth. Cambridge Univ. Press.

Katsura, T., Yokoshi, S., Kawabe, K., Shatskiy, A., Geeth, M.A., Manthilake, M., Zhai, S., Fukui, H., Chamathni, H.A., Hegoda, I., Yoshino, T., Yamazaki, D., Matsuzaki, T., Yoneda, A., Ito, E., Sugita, M., Tomioka, N., Hagiya, K., Nozawa, A., Funakoshi, K., 2009. P–V–T relations of $MgSiO_3$ perovskite determined by in situ X-ray diffraction using a large-volume high-pressure apparatus. Geophys. Res. Lett. 36, L01305. doi:10.1029/2008GL035658.

Keppler, H., Dubrovinsky, L., Narygina, O., Kantor, I., 2008. Optical absorption and radiative thermal conductivity of silicate perovskite to 125 GPa. Science 322. doi:10.1126/science.1164609.

Kido, M., Čadek, O., 1997. Inferences of viscosity from the oceanic geoid: indication of a low viscosity zone below the 660-km discontinuity. Earth Planet. Sci. Lett. 151, 125–137.

King, S.D., Masters, G., 1992. An inversion for radial viscosity structure using seismic tomography. Geophys. Res. Lett. 19, 1551–1554.

Leitch, A.M., Yuen, D.A., 1989. Internal heating and thermal constraints on the mantle. Geophys. Res. Lett. 16, 1407–1410.

Li, J., Struzhkin, V.V., Mao, H.K., Shu, J.F., Hemley, R.J., Fei, Y.W., Mysen, B., Dera, P., Prakapenka, V., Shen, G.Y., 2004. Electronic spin state of iron in lower mantle perovskite. Proc. Natl. Acad. Sci. 101, 14027–14030.

Li, J., Sturhahn, W., Jackson, J.M., Struzhkin, V.V., Lin, J.F., Zhao, J., Mao, H.K., Shen, G., 2006. Pressure effect on the electronic structure of iron in (Mg,Fe)(Si,Al)O-3 perovskite: a combined synchrotron Mossbauer and X-ray emission spectroscopy study up to 100 GPa. Phys. Chem. Mineral. 33, 575–585.

Li, L., Weidner, D.J., 2008. Effect of phase transitions on compressional-wave velocities in the Earth mantle. Nature 454, 984.

Lin, J.F., Struzhkin, V.V., Jacobsen, S.D., Hu, M.Y., Chow, P., Kung, J., Liu, H.Z., Mao, H.K., Hemley, R.J., 2005. Spin transition of iron in magnesiowustite in the Earth's lower mantle. Nature 436, 377–380.

Lin, J.F., Weir, S.T., Jackson, D.D., Evans, W.J., Vohra, Y.K., Qiu, W., Yoo, C.S., 2007a. Electrical conductivity of the lower-mantle ferropericlase across the electronic spin transition. Geophys. Res. Lett. 34, L16305.

Lin, J.F., Vanko, G., Jacobsen, S.D., Iota, V., Struzhkin, V.J.F., Vanko, G., Jacobsen, S.D., Iota, V., Struzhkin, V.V., Prakapenka, V.B., Kuznetsov, A., Yoo, C.S., 2007b. Spin transition zone in Earth's lower mantle. Science 317, 1740–1743.

Lin, J.F., Tsuchiya, T., 2008. Spin transition of iron in the Earth's lower mantle. Phys. Earth Planet. Int. 170, 248–259.

Lin, J.F., Watson, H., Vanko, G., Alp, E.E., Prakapenka, V.B., Dera, P., Struzhkin, V.V., Kubo, A., Zhao, J.Y., McCammon, C., Evans, W.J., 2008. Intermediate-spin ferrous iron in lowermost mantle post-perovskite and perovskite. Nature Geosci. 1, 688–691.

Lin, J.F., Wenk, H.R., Voltolini, M., Speziale, S., Shu, J.F., Duffy, T.S., 2009. Deformation of lower-mantle ferropericlase (Mg,Fe)O across the electronic spin transition. Phys. Chem. Min. 36, 585–592.

Matyska, C., Moser, J., Yuen, D.A., 1994. The potential influence of radiative heat transfer on the formation of megaplumes in the lower mantle. Earth Planet. Sci. Lett. 125, 255–266.

Matyska, C., Yuen, D.A., 2001. Are mantle plumes adiabatic? Earth Planet. Sci. Lett. 189, 165–176.

Matyska, C., Yuen, D.A., 2005. The importance of radiative heat transfer on superplumes in the lower mantle with the new post-perovskite phase change. Earth Planet. Sci. Lett. 234, 71–81.

Matyska, C., Yuen, D.A., 2006. Lower mantle dynamics with the post-perovskite phase change, radiative thermal conductivity, temperature- and depth-dependent viscosity. Phys. Earth Planet. Inter. 154, 196–207.

Matyska, C., Yuen, D.A., 2007. Lower-mantle material properties and convection models of multiscale plumes. In: Foulger, G.R., Jurdy, D.M. (Eds.), Plates, Plumes, and Planetary Processes, Geological Society of America Special Paper 430, pp. 137–163.

McCammon, C., 1997. Perovskite as a possible sink for ferric iron in the lower mantle. Nature 387, 694–696.

McCammon, C., Kantor, I., Narygina, O., Rouquette, J., Ponkratz, U., Sergueev, I., Mezouar, M., Prakapenka, V., Dubrovinsky, L., 2008. Stable intermediate-spin ferrous iron in lower-mantle perovskite. Nature Geosci. 1, 687–688.

McKenzie, D.P., 1966. The viscosity of the lower mantle. J. Geophys. Res. 71, 3995–4010.

Mitrovica, J.X., Forte, A.M., 2004. A new inference of mantle viscosity based upon joint inversion of convection and glacial isostatic adjustment data. Earth Planet. Sci. Lett. 225, 177–189.

Morra, G., Yuen, D.A., Boschi, L., Chatelain, P., Koumoutsakos, P., Tackley, P.J., 2010. The fate of the slabs interacting with a viscosity hill in the mid-mantle. Phys. Earth. Planet. Int. 180, 271–282.

Nakagawa, T., Tackley, P.J., 2004. Effects of a perovskite-post perovskite phase change near core-mantle boundary in compressible mantle convection. Geophys. Res. Lett. 31, L16611.

Naliboff, J.B., Kellogg, L.H., 2006. Dynamic effects of a step-wise increase in thermal conductivity and viscosity in the lowermost mantle. Geophys. Res. Lett. 33, L12S09.

O'Farrell, K.A., Lowman, J.P., 2010. Emulating the thermal structure of spherical shell convection in plane-layer geometry mantle convection models. Phys. Earth Planet. Int. 182, 73–84.

Peltier, W.R., Andrews, J.T., 1976. Glacial-isostatic adjustment-I. The forward problem. Geophys. J.R. Astr. Soc. 46, 605–646.

Ranalli, G., 1995. Rheology of the Earth. Chapman and Hall, London, 413 p..

Ricard, Y., Wuming, B., 1991. Inferring viscosity and the 3-D density structure of the mantle from geoid, topography and plate velocities. Geophys. J. Int. 105, 561–572.

Sabadini, R., Yuen, D.A., Boschi, E., 1982. Polar wandering and the forced responses of a rotating, multi-layered viscoelastic planet. J. Geophys. Res. 87, 2885–2903.

Sammis, C.G., Smith, J.C., Schubert, G., Yuen, D.A., 1977. Viscosity-depth profile of the Earth's mantle: effects of polymorphic phase transitions. J. Geophys. Res. 82, 3747–3761.

Schubert, G., Masters, G., Tackley, P., Olson, P., 2004. Superplumes or plume clusters? Phys. Earth Planet. Inter. 146, 147–162.

Schubert, G., Turcotte, D.L., Olson, P., 2001. Mantle Convection in the Earth and Planets. Cambridge Univ. Press.

Shahnas, M.H., Peltier, W.R., Wu, Z., Wentzcovitch, R., 2011. The high pressure electronic spin transition in iron: impacts upon mantle mixing. J. Geophys. Res. doi:10.1029/2010JB007965.

Soldati, G., Boschi, L., Deschamps, F., Giardini, D., 2009. Inferring radial models of mantle viscosity from gravity (GRACE) data and an evolutionary algorithm. Phys. Earth. Planet. Int. 176, 19–32.

Stackhouse, S., Brodholt, J.P., Price, G.D., 2007. Electronic spin transitions in iron-bearing $MgSiO_3$ perovskite. Earth. Planet. Sci. Lett. 253, 282–290.

Steinbach, V.C., Hansen, U., Ebel, A., 1989. Compressible convection in the Earth's mantle: a comparison of different approaches. Geophys. Res. Lett. 16, 633–636.

Tackley, P.J., Nakagawa, T., Hernlund, J.W., 2007. Influence of the post-perovskite transition on thermal and thermo-chemical mantle convection. In: Hirose, K., Brodholt, J., Lay, T., Yuen, D.A. (Eds.), Post-Perovskite: The Last Mantle Phase Transition, Geophysical Monograph Series 174, American Geophysical Union, pp. 229–247.

Tarduno, J., Bunge, H.P., Sleep, N., Hansen, U., 2009. The Bent Hawaiian-Emperor hotspot track: inheriting the mantle wind. Science 324, 51–53.

Tosi, N., Čadek, O., Martinec, Z., Yuen, D.A., Kaufmann, G., 2009. Is the long-wavelength geoid sensitive to the presence of post-perovskite above the core-mantle boundary? Geophys. Res Lett. 36, L05303.

Tosi, N., Sabadini, R., Marotta, A.M., Vermeersen, L.A., 2005. Simultaneous inversion for the Earth's mantle viscosity and ice mass imbalance in Antarctica and Greenland. J. Geophys. Res. 110. doi:10.1029/2004JB003236.

Tsuchiya, T., Wentzcovitch, R.M., da Silva, C.R.S., de Gironcoli, S., 2006a. Spin transition in magnesiowustite in earth's lower mantle. Phys. Rev. Lett. 96, 198501.

Tsuchiya, T., Wentzcovitch, R.M., da Silva, C.R.S., de Gironcoli, S., Tsuchiya, J., 2006b. Pressure induced high spin to low spin transition in magnesiowüstite. Phys. Stat. Sol. (B) 243, 2111–2116.

Umemoto, K., Wentzcovitch, R., Yonggang, G.Y., Requist, R., 2008. Spin transition in $(Mg,Fe)SiO_3$ perovskite under pressure. Earth Planet. Sci. Lett. 276, 198–206.

Umemoto, K., Hsu, H., Wentzcovitch, R.M., 2010. Effect of site degeneracies on the spin crossovers in $(Mg, Fe)SiO_3$ perovskite. Phys. Earth Planet. Int. 180, 209–214.

van Keken, P., Yuen, D.A., 1995. Dynamical influences of high viscosity in the lower mantle induced by the steep melting curve of perovskite. J. Geophys. Res. 100, 15233–15248.

Wentzcovitch, R.M., Justo, J.F., Wu, Z., da Silva, C.R.S., Yuen, D.A., Kohlstedt, D., 2009. Anomalous compressibility of ferropericlase throughout the iron spin cross-over. Proceedings of the National Academy of Sciences of the United States of America 106, 8447–8452.

Wu, Z., Justo, J.F., da Silva, C.R.S., de Gironcoli, S., Wentzcovitch, R.M., 2009. Anomalous thermodynamic properties in ferropericlase throughout its spin crossover transition. Phys. Rev. B 80, 014409.

Yamazaki, D., Karato, S., 2001. Some mineral physics constraints on rheology and geothermal structure of earth's lower mantle. Am. Mineral. 86, 358–391.

Yamazaki, D., Yoshino, T., Ohfuji, H., Ando, J., Yoneda, A., 2006. Origin of seismic anisotropy in the D''-layer inferred from shear deformation experiments on post-perovskite phase. Earth Planet. Sci. Lett. 252, 372–378.

Yuen, D.A., Sabadini, R., 1985. Viscosity stratification of the lower mantle as inferred from the J2 observation. Ann. Geophys. 3, 647–654.

Yuen, D.A., Čadek, O., van Keken, P., Reuteler, D.M., Kývalová, H., Schroeder, B.A., 1996. Combined results for mineral physics, tomography and mantle convection and their implications on global geodynamics. In: Boschi, E., Ekström, G., Morelli, A. (Eds.), Seismic Modelling of the Earth's Structure, Editrice Compositori, Bologna, Italy, pp. 463–506.

Zerr, A., Boehler, R., 1994. Constraints on the melting temperature of the lower mantle from high-pressure experiments on MgO and magnesiowüstite. Nature 371, 506–508.

Zhang, F.W., Oganov, A.R., 2006. Valence state and spin transitions of iron in Earth's mantle silicates. Earth. Planet. Sci. Lett. 249, 436–443.